RADIO SCIENCE, VOL. 44, RS5015, doi:10.1029/2008RS004095, 2009

Wideband MIMO channel characterization in TV studios and inside buildings in the 2.2–2.5 GHz frequency band

N. Razavi-Ghods[1] and S. Salous[2]

Received 16 November 2008; revised 10 June 2009; accepted 3 August 2009; published 28 October 2009.

[1] Multiple input multiple output (MIMO) measurements were performed with a chirp sounder with a switched antenna array at the transmitter and eight parallel receiver channels with 96-MHz bandwidth at 2.25 GHz in TV studios and 240-MHz bandwidth at 2.38 GHz inside buildings. MIMO capacity was estimated from the data with linear and circular arrays with array sizes 2 by 2, 4 by 4, and 6 by 8. Mean capacity estimates for 30-dB signal-to-noise ratio for both line of sight and obstructed line of sight were on the order of 11–31 b/s/Hz for the 2 by 2 to 4 by 4 antenna configurations and for the 6 by 8 directional antenna measurements a median capacity of 50 b/s/Hz. This is an increase of 20 b/s/Hz from the 4 by 4 omnidirectional antenna array indicating diversity gain as well as an increase due to the number of antennas.

Citation: Razavi-Ghods, N., and S. Salous (2009), Wideband MIMO channel characterization in TV studios and inside buildings in the 2.2–2.5 GHz frequency band, *Radio Sci.*, *44*, RS5015, doi:10.1029/2008RS004095.

1. Introduction

[2] Multipath propagation in radio channels has long been considered the main impairment for high data rate transmission. The presence of multipath in a time varying environment causes intersymbol interference, frequency selectivity and time fading. Examples of techniques that limit these effects include diversity (antenna, frequency and time), smart antennas, coding and modulation schemes such as orthogonal frequency division multiplexing (OFDM). While these techniques attempt to combat the effects of multipath, an alternative technique, which exploits the presence of multipath to enhance the data rate in a limited spectrum was proposed by *Winters* [1987] and *Foschini* [1996]. The technique widely termed as multiple input multiple output (MIMO) uses multiple transmit and multiple receive antennas and relies on the decorrelation of the radio channels between the antenna elements to transmit parallel data streams. The concept of MIMO was first introduced by *Winters* [1987] for two basic communication systems. The first was for communication between multiple mobiles and a base station with multiple antennas and the second was for communication between two mobiles each with multiple antennas. Subsequently, the papers of *Foschini* [1996] and *Foschini and Gans* [1998] presented the analytical basis of MIMO systems and proposed two suitable architectures for its realization known as vertical BLAST, and diagonal BLAST. The basic motivation was to increase the data rate in a constrained spectrum. The initial application of MIMO was envisaged for indoor WLAN, fixed wireless access networks, wireless local loop, and building-to-building wireless communications. Later other applications were proposed such as metropolitan voice/data wireless networks (UMTS, EDGE, and fourth-generation networks), very high speed fixed and mobile wireless (point to multipoint), acoustic communications, and broadcast systems (HDTV).

[3] For ideal conditions, that is independent and identically distributed (IID) flat Rayleigh fading channels between the different antenna elements and constrained total power, such a technique is expected to increase the data rate linearly with the number of receive antennas [*Foschini*, 1996]. In addition, the data are transmitted in bursts, such that the channel can be assumed quasi-stationary and that the channel is known at the receiver through the transmission of a training sequence [*Hassibi and Hochwald*, 2003] but not necessarily at the transmitter. MIMO is a narrowband concept where the assumption of flat fading holds, and therefore, the majority of the channel capacity expressions are given for the narrowband case. Essential to this assumption is the measurement of the coherent bandwidth of the channel. The wideband case or the frequency selective channel represents the average capacity of the narrowband channels across the bandwidth, which can provide frequency diversity. However, real radio channels can deviate

[1]Cavendish Laboratory, University of Cambridge, Cambridge, UK.
[2]School of Engineering, Durham University, Durham, UK.

0048-6604/09/2008RS004095$11.00

significantly from the IID model and the channel capacity can vary significantly with the antenna array type and geometry. Therefore, experimental characterization of such propagation channels is fundamental to the deployment of MIMO technologies.

[4] Through a number of indoor MIMO measurements we aim to examine some of the characteristics of the wideband time-variant MIMO channels for two different bandwidths in the 2.2–2.5 GHz band using different antenna configurations. The two frequency bands are intended for wideband digital video broadcasting systems and for the Industrial, Scientific and Medical (ISM) band which supports a number of wireless standards for wireless local access networks primarily proposed for indoor office and home environments. The environments under test were chosen to cover a variety of propagation conditions such as line of site (LOS) and obstructed line of site (OLOS) in three of the BBC TV studios and the School of Engineering at Durham University, which is representative of an indoor to indoor environment.

[5] The paper briefly describes the sounder used in the measurements including the antenna arrays, the processing of the data and presents results for capacity estimated for different antenna configurations. Capacity variations as a function of distance on a grid of 8 by 8 m show the variations in the studio environment every 2 m. The correlation between capacity and angular spread at both ends of the link is obtained from double directional measurements from the 6 by 8 directional antenna arrays. In addition, as OFDM MIMO is a strong candidate for fourth-generation systems, second-order statistics such as level crossing per MHz and average bandwidth of frequency selectivity are presented.

2. Measurement System

[6] The measurements were performed using a custom designed chirp channel sounder which uses direct digital frequency synthesizers (DDFS) for the generation of the chirp signal at both the transmitter and receiver. The chirp technique which has been long used for radar and ionospheric sounding has the advantage of avoiding high peak transmission power, high bandwidths with bandwidth compression through the use of heterodyne detection and flexibility in processing the acquired data with different time and frequency resolutions [*Salous*, 1986]. Application to mobile radio channel measurements became feasible with the introduction of high-speed synthesizers (DDFS) and large field programmable gate arrays which enabled the design of a compact signal generator [*Salous et al.*, 1998]. The DDFS avoids the fly back transients of phased locked loops and provides wide transmission bandwidths at high waveform repetition frequency (WRF) necessary to accommodate the high Doppler shifts in mobile radio environments. The bandwidth compression at the receiver enables the use of low data acquisition rates and multiple receive channels [*Salous and Hinostroza*, 2005; *Salous et al.*, 2005a]. The sounder used in the measurements combines the 400 MHz wide bandwidth synthesizer reported by *Salous and Hinostroza* [2005] with the parallel receive architecture of *Salous et al.* [2005b]. The updated sounder has a programmable chirp bandwidth up to 240 MHz and waveform repetition frequency (WRF) up to 250 Hz for single input single output configurations. It has a single input multiple output (SIMO) architecture where the transmitter has a single output and the receiver has eight parallel receive channels (see Figure 1a). MIMO measurements are enabled by employing a fast switch to sequentially transmit on each antenna for the duration of a single chirp waveform. To identify the sequence of transmission the switch has an idle state as shown in Figure 1b. Hence for n_T transmit antenna array, the repetition rate of the sounding is reduced by a factor equal to $n_T + 1$.

[7] The present configuration can accommodate up to 8 by 8 MIMO measurements and provides a minimum unambiguous Doppler coverage of ±25 Hz for four transmit antennas with a WRF of 250 Hz. For indoor environments this is sufficient as 25 Hz Doppler shift corresponds to a maximum walking speed of 3.75 m/s. Dual band 4 by 4 MIMO measurements at 2.2 GHz and 5.8 GHz are enabled through up and down converters [*Salous et al.*, 2005b]. Calibration data are collected in addition to the measurement data in order to compensate for the differing channel gains in postprocessing.

[8] The measurements reported here were performed with 4 by 4 discone antenna arrays designed for the frequency range between 2.1 and 6 GHz with different configurations including uniform linear array and circular array as shown in Figure 2a. The discone antennas were calibrated at 2 GHz in an anechoic chamber using a specially designed quadrature unit to measure the magnitude and the phase [*Feeney*, 2007]. The polar diagram for the four-element discone ULA is shown in Figure 2b, while the polar diagram for one of the elements of the UCA is displayed in Figure 2c with element 4 of the ULA with $\lambda/2$. Figures 2b and 2c show that the different elements affected each others radiation pattern as the array was rotated. This is expected as the elements obstructed each other for certain angles of arrival/angles of departure.

[9] The measurements in the ISM band (2.38 GHz) were all performed indoor on two floors in the School of Engineering at Durham University as shown in Figure 3. The measurements were collected with 240 MHz bandwidth and the following antenna configurations: (1) Floors 2a and 3a: 2 transmit by 2 receive (10250 impulse responses), 3 transmit by 3 receive (9500 impulse responses), and 4 transmit by 4 receive (11000 impulse

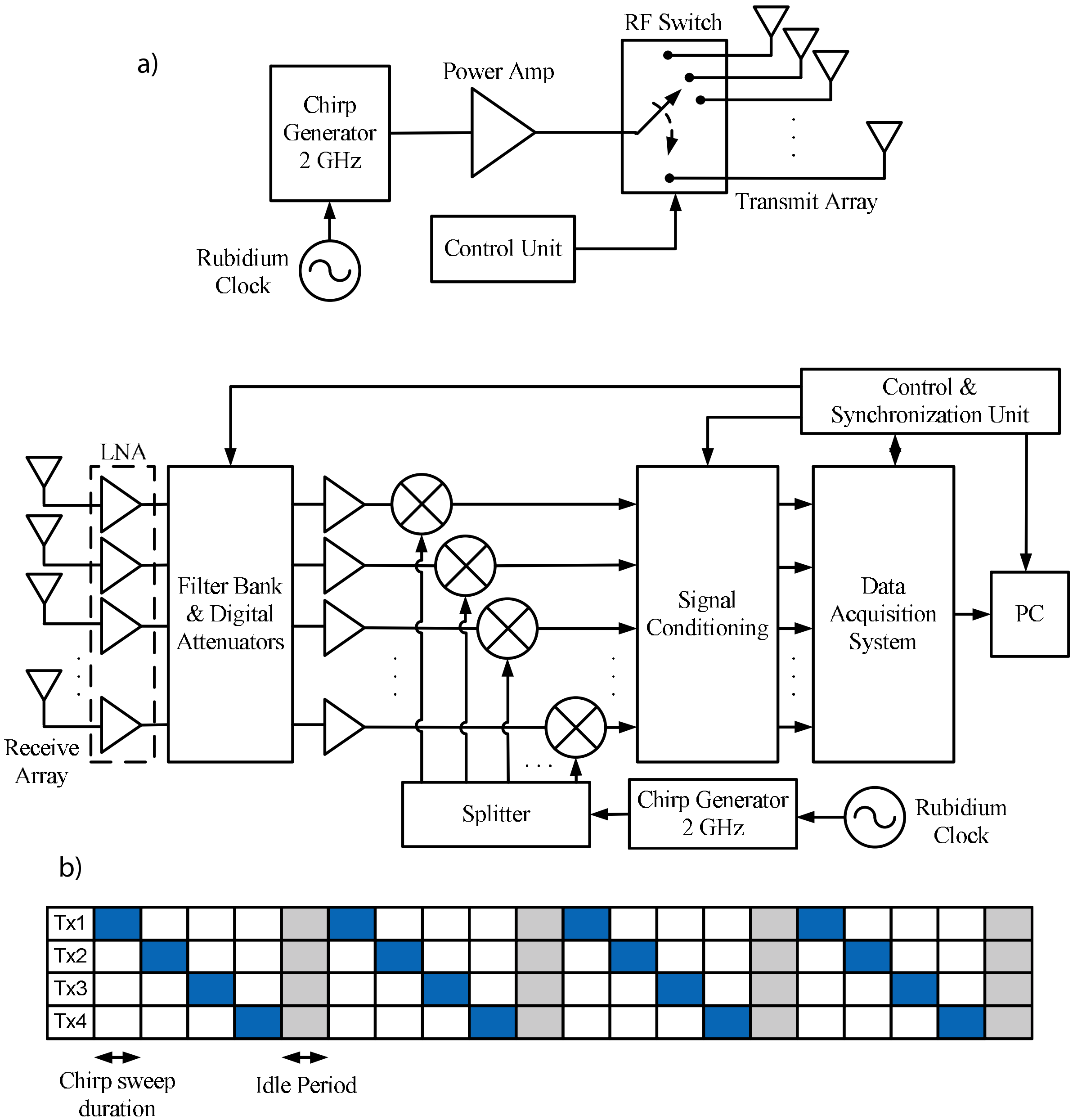

Figure 1. (a) Architecture of the sounder at 2 GHz and (b) switching antenna pattern for four transmit antennas.

responses) all with ULA; 4 transmit (UCA) 2 receive ULA (10000 impulse responses); 2, and 3 transmit ULA by 4 receive UCA (10000, and 5500 impulse responses, respectively). (2) Floors 2a and 2b: 4 transmit by 4 receive UCA (11000 impulse responses).

[10] Another set of measurements was performed in the School of Engineering floor 2b, using 6 by 8 antenna arrays with directional arrays at both ends of the link designed to provide full 360° coverage. The data were processed for both MIMO capacity and for angular spread information to study the relationship between MIMO capacity and angular spread at both ends of the radio link. The 6 array element and its radiation pattern are shown in Figures 2d and 2e. All the antenna arrays used in the measurements reported herein have vertical polarization. The mutual coupling in the horizontal and

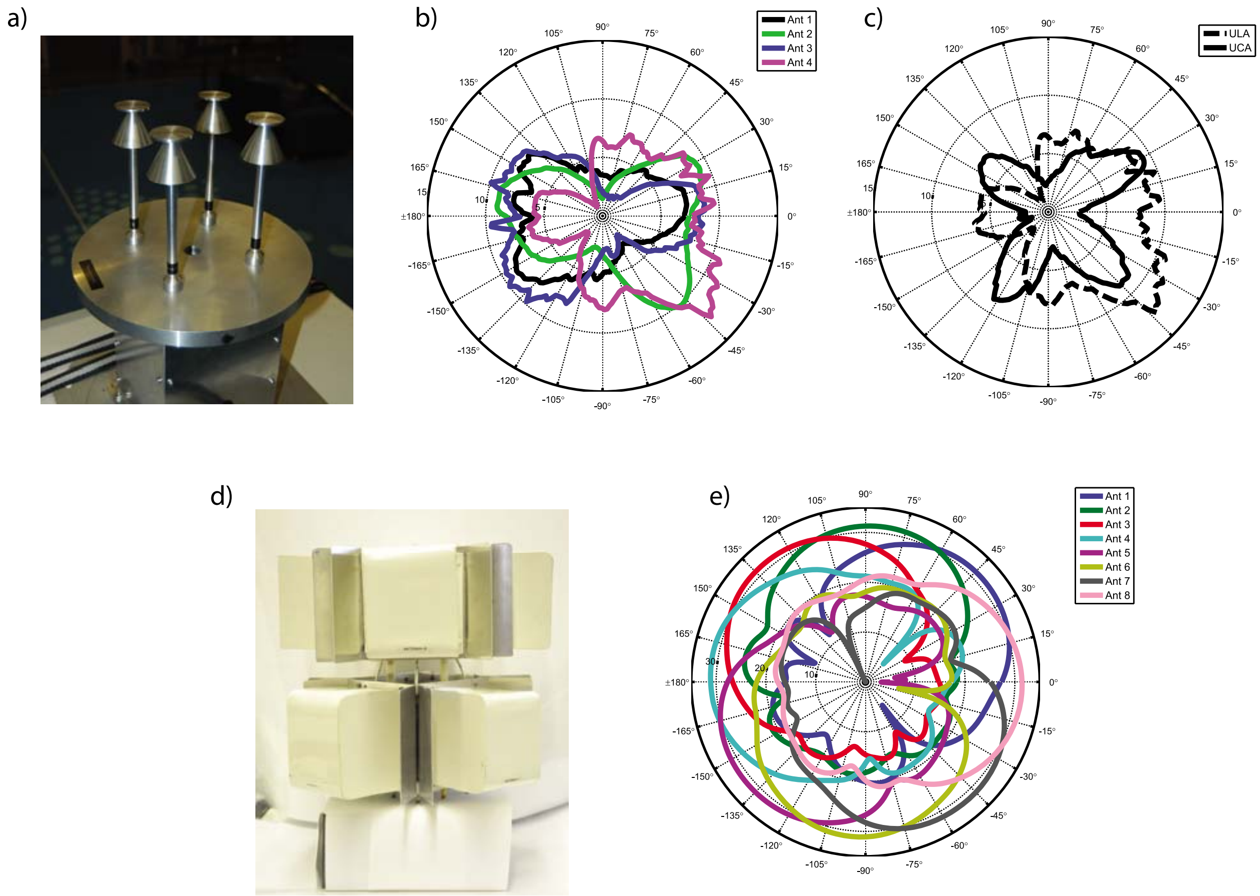

Figure 2. (a) Uniform circular array (UCA) of discone antennas, (b) radiation pattern of discone uniform linear array (ULA), (c) single element from the ULA and UCA, (d) six-element patch array, and (e) its directional radiation pattern.

vertical planes between the antenna elements for the 6 and 8 element directional arrays was measured to be better than -19 dB. For the dicsone arrays, the mutual coupling was measured to be -17 to -18 dB in the band of interest.

[11] The data were acquired in blocks of 1 s, which consisted of 250 impulse responses simultaneously on eight channels. The environment of the TV studio measurements is shown in Figure 4 where a total of 37500 impulse responses were collected using the 4 ULA by 4 UCA discone array with 96 MHz bandwidth at 2.25 GHz.

3. Data Processing

3.1. Sounder General Processing

[12] The data can be processed to estimate a number of channel functions as required. In the present study the time variant transfer function, the power delay profile, and the delay Doppler function were determined. In the chirp sounder, the received IF output of each receive channel consists of beat notes for each multipath component. For MIMO operation, the data are initially demultiplexed, and then spectrum analyzed using the fast Fourier transform to obtain the time variant impulse function. In this stage only half of the data points are saved due to the even symmetry. A second FFT performed on each complex impulse function yields the complex time variant transfer function, whereas a second FFT on each time delay bin gives the time delay versus Doppler spectrum.

3.2. MIMO Capacity Estimation

[13] The MIMO channel matrix data acquired from the measurements can be represented as a four-dimensional complex transfer function matrix, **H**, the size of which is

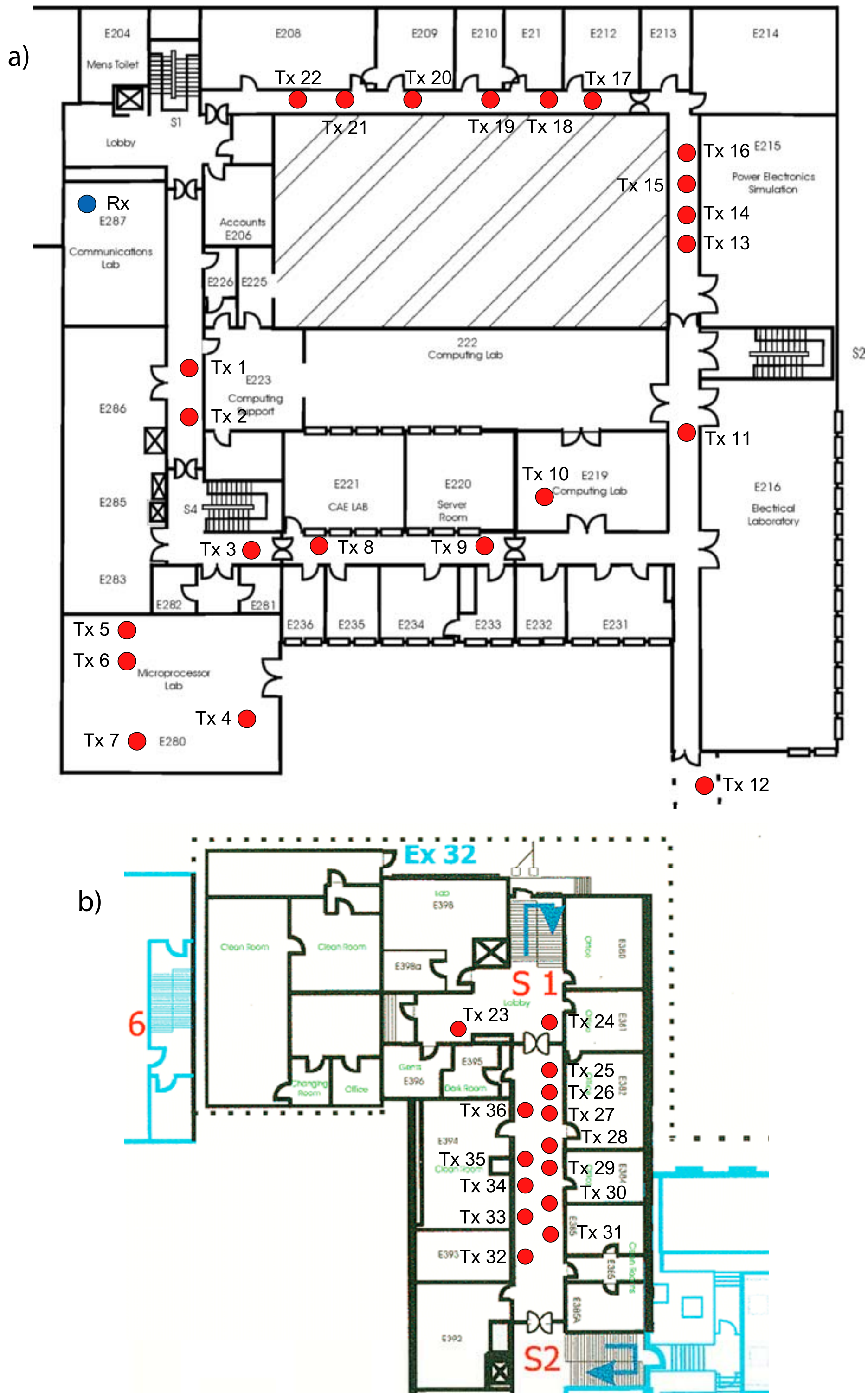

Figure 3. Layout of floors (a) 2 and (b) 3 in the School of Engineering, Durham University.

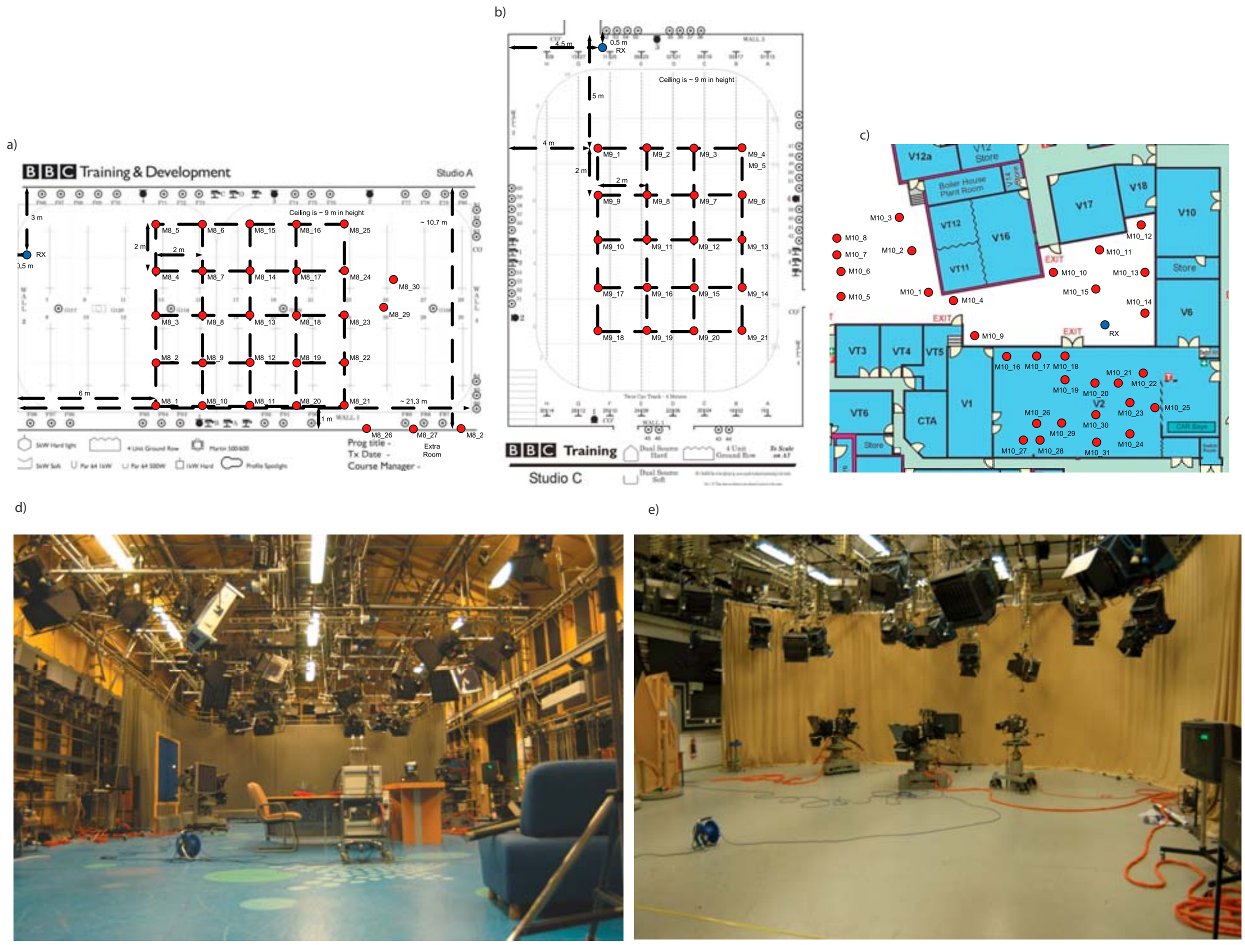

Figure 4. Layout and photographs of the measurement environment in the BBC studio. (a) Measurement grid in Studio A, (b) measurement grid in Studio C, (c) measurement layout and locations in BBC lab, and (d and e) photographs of studios.

given by $n_R \times n_T \times N_f \times N_t$, where n_T and n_R represent the number of antennas at the transmitter and at the receiver, respectively, and the parameters N_t and N_f are used to define the number of channel responses in time and the total number of frequency points in the transfer function of the channel, respectively. The data were acquired while the receiver was not in motion over 1 s time intervals with an average of 50 sweeps per antenna. The capacity estimates therefore represent a time average rather than a spatial average.

[14] The evaluation of link capacity can provide a measure of the channel's upper bound limit on achievable data rate. The capacity of a frequency selective MIMO channel can be expressed as the average of N_f frequency flat subchannels as given in equations (1) and (2) where equation (2) is the average of the conventional MIMO capacity expression for narrowband channels [*Paulraj et al.*, 2003].

$$C_{WB} \approx \frac{1}{N_f} \sum_{i=1}^{N_f} C_{NB}^{(i)} \tag{1}$$

$$C_{WB} = \frac{1}{N_f} \sum_{i=1}^{N_f} \log_2 \left[\det \left(I_{n_R} + \frac{\rho}{n_T} H_i H_i^H \right) \right] \tag{2}$$

where ρ denotes the average signal-to-noise ratio (SNR) and $\mathbf{H}_i$ is the $n_R \times n_T$ matrix containing the sampled channel transfer functions for each of the subchannels.

[15] Prior to the computation of the channel capacity, the MIMO channel matrix data are normalized to remove

the absolute power bias in order to compare the results in different environments. In this study the channel matrices were normalized so that the Frobenius norm is equal to $n_R n_T$, which gives an average SISO gain of one [*Jenson and Wallace*, 2004]. Normalization of each individual sampled channel matrix to have a SISO gain of one, assumes some form of power control, which allows the receiver to always have the same SNR, regardless of path loss. A more practical approach estimates an average of one over all SISO gains, thus assuming an average SNR. If β represents the normalization constant for each time snapshot and f_n represents the frequency sample index (frequency bin), the specified unity power gain constraint may be expressed as [*Wallace et al.*, 2003]

$$\frac{1}{N_f \cdot n_R n_T} \sum_{f_n=1}^{N_f} \sum_{i=1}^{n_R} \sum_{j=1}^{n_T} \left| \beta \hat{H}_{ij}^{(f_n)} \right|^2 = 1 \tag{3}$$

Solving for β gives

$$\beta = 1 \Big/ \sqrt{\left(\frac{1}{N_f \cdot n_R n_T} \sum_{f_n=1}^{N_f} \sum_{i=1}^{n_R} \sum_{j=1}^{n_T} \left| \hat{H}_{ij}^{(f_n)} \right|^2 \right)} \tag{4}$$

3.3. Correlation Analysis

[16] MIMO channel capacity is dependent on the correlation between the different antenna elements at both ends of the link [*Loyka*, 2001; *Loyka and Kouki*, 2001]. Here, the correlation coefficients are defined using $H_{i,j}^{(k)}$, which is the k^{th} channel frequency bin in each transfer function from the j^{th} transmit element to the i^{th} receive element [*Maharaj et al.*, 2005; *Eugene et al.*, 2004]. Therefore the correlation coefficient at the receiver with particular element spacing is defined as

$$\gamma_{d,RX} = \frac{\sum_{k=1}^{N_f} \sum_{j=1}^{n_T} \sum_{i=1}^{n_R-d} H_{i,j}^{(k)} H_{i+d,j}^{(k)*}}{\sqrt{\left(\sum_{k=1}^{N_f} \sum_{j=1}^{n_T} \sum_{i=1}^{n_R-d} \left| H_{i,j}^{(k)} \right|^2 \right) \left(\sum_{k=1}^{N_f} \sum_{j=1}^{n_T} \sum_{i=1}^{n_R-d} \left| H_{i+d,j}^{(k)} \right|^2 \right)}} \tag{5}$$

where d is the element spacing, typically defined as 1. The transmit correlation coefficient is calculated by interchanging the roles of the transmitter and receiver [*Maharaj et al.*, 2005].

3.4. Angular and Time Delay Spread

[17] The 6 by 8 data were analyzed using the SAGE algorithm [*Fleury et al.*, 1999] to estimate the angle of departure and angle of arrival. Since the data were acquired with a high time delay resolution sounder, the time delay estimate was obtained from the power delay profile, i.e., after the first FFT. Multipath components within a certain threshold level from the maximum of the profile were selected and their time delays were entered into the SAGE algorithm. The algorithm then estimated the angle of arrival or angle of departure of these multipath components and their signal strength. The data were calibrated prior to the use of the estimation of angular information for antenna gain and for channel gains between the different receive channels. An example is shown in Figure 5a for the 6 by 8 antenna array measurement. The angular information was subsequently used to estimate the RMS angular spread at both ends of the link. The data were also processed for RMS time delay spread for 20 dB threshold level for each receive antenna, and the average from all the antennas was then obtained.

4. Measurement Results

4.1. ISM Band

4.1.1. Results for Discone Antenna Arrays

[18] An example of the delay/Doppler function for a LOS 4 by 4 is displayed in Figure 5b which shows a delay spread of about 50 ns and 8 Hz Doppler for a moving receiver. The estimated mean RMS time delay spread for these measurements varied between 22 and 29 ns for the different antenna configurations.

[19] The MIMO capacity for the different antenna configurations was computed for 2 by 2, 2 by 4, 3 by 3, 3 by 4, 4 by 2 and 4 by 4 from repeated field trials. The results for the cumulative distribution of capacity for 30 dB SNR are displayed in Figure 6a with the capacity as a function of SNR in Figure 6b (see Table 1 for summary of the median capacity).

[20] Figure 6a shows that for the same number of transmit and receive antennas, a nearly linear increase in capacity is achieved (the median capacity is 16.65, 23.88 and 31.2 b/s/Hz for 2 by 2, 3 by 3 and 4 by 4). The effect of antenna diversity is shown to increase the capacity. For example for the 2 by 4 antenna configuration the median capacity was 20.1 b/s/Hz, which increased to 26.7 b/s/Hz for the 3 by 4 antenna configurations. Comparing the 2 by 4 and the 4 by 2 median capacity it is seen that a reduction of 2 b/s/Hz has occurred in the latter, which is contrary to normal expectation since the mobile radio channel is ideally reciprocal. However, this reduction can be attributed to the transmit switch isolation which was measured to be only 20 dB. This highlights the benefit of using separate receiver channels as opposed to a single switched receiver channel as commonly used in fully sequential sounders [*Schwarz et al.*, 1993]. The results in this section confirm that an indoor environment provides suitable multiplexing capacity gain. The added capacity

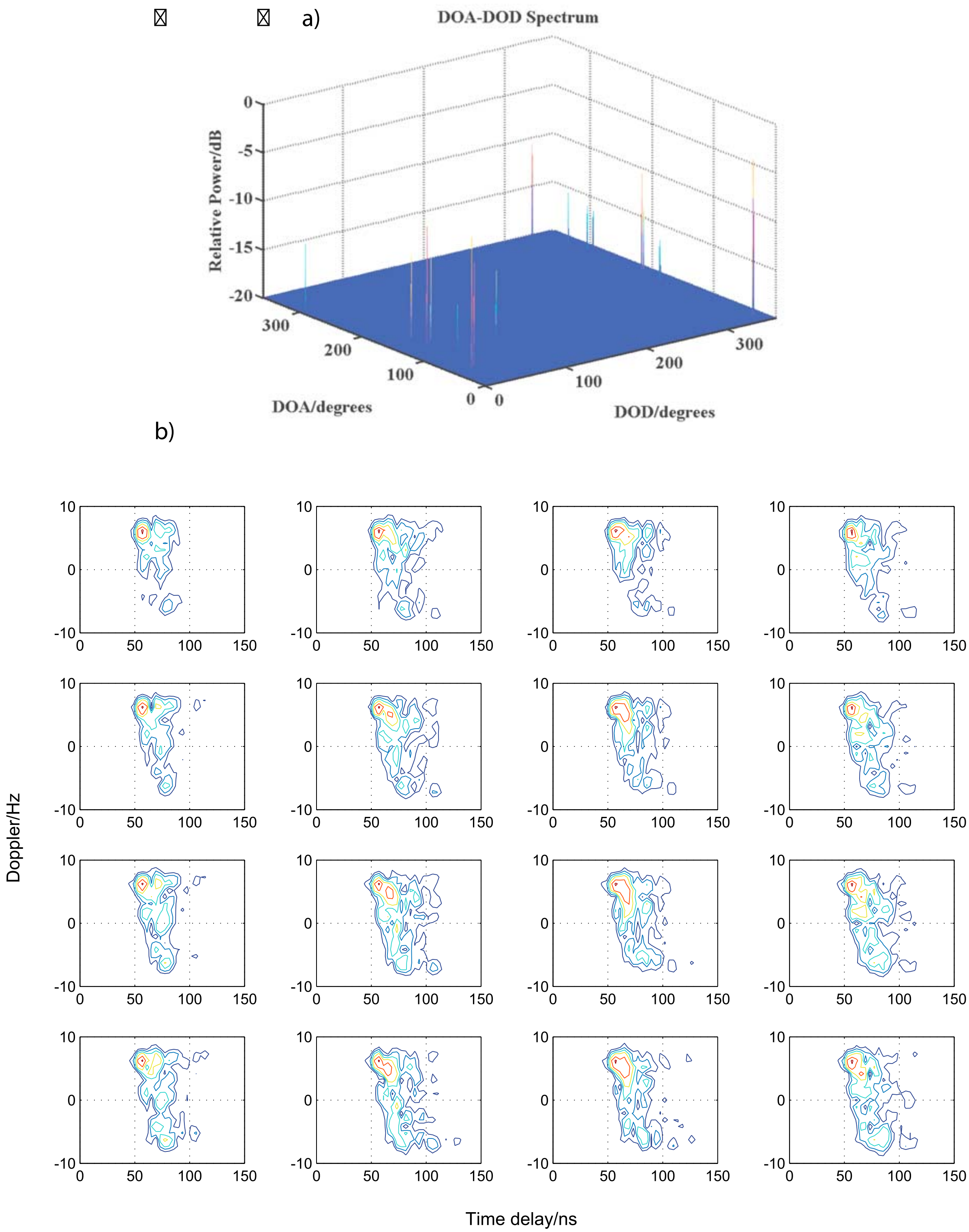

Figure 5. (a) Angle of departure/angle of arrival extracted from 6 by 8 measurement. (b) Delay Doppler function for 4 by 4 antenna array in the 2.25-GHz band in the BBC studio.

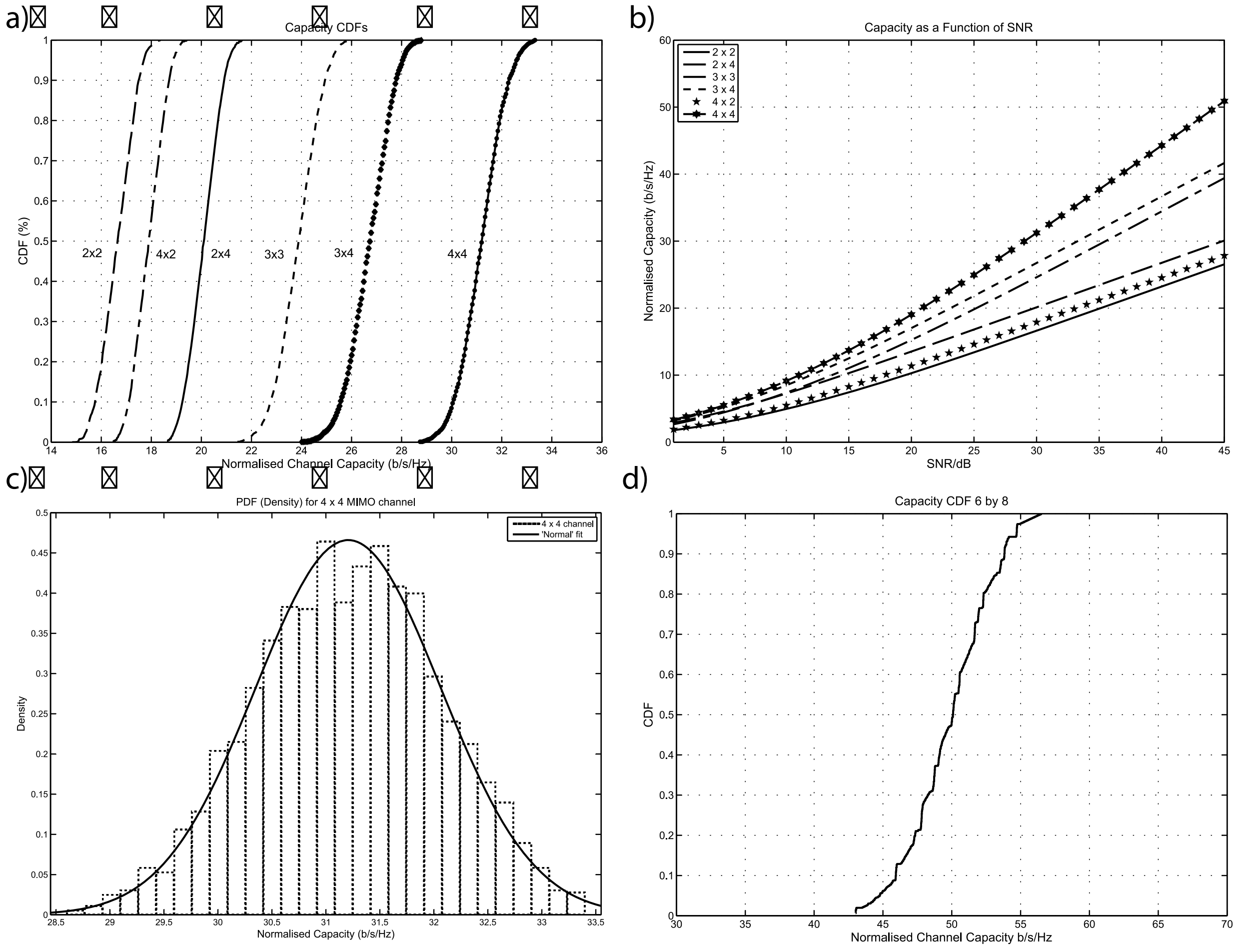

Figure 6. Capacity estimates in the ISM band for 2 by 2 up to 4 by 4 (a) CDF of capacity for 30 dB SNR, (b) capacity as a function of SNR, (c) PDF of capacity for 30 dB SNR fitted with a normal distribution, and (d) capacity estimates derived for the 6 by 8 directional antennas.

due to diversity gain can be seen from Figure 6b where for example for a 20 b/s/Hz capacity, a saving of 2.5 dB/antenna is obtained. In Figure 6c a normal distribution, overlaid on the probability density function for the 4 by 4 MIMO capacity displayed in Figure 6a is seen to provide an appropriate fit to the data.

[21] To study the effect of antenna separation, a set of data files collected at 10 different locations with antenna spacing equal to $\lambda/3$, $\lambda/2$, λ and $3\lambda/2$ were analyzed. The capacity and correlation coefficient at both ends of the link were computed. The results indicate that an increase in capacity is achieved as the antenna elements separation is increased. For $\lambda/3$ spacing the capacity is on average reduced by 2 b/s/Hz as compared to $\lambda/2$ spacing. This could be attributed to a reduction in spatial correlation and reduced coupling between the antenna elements.

Table 1. Mean Capacity Estimates for the Two Frequency Bands in the TV Studio

Antenna Configuration	Mean Capacity (bits/s/Hz)
BBC 2 × 2 LOS	11.7
BBC 2 × 2 OLOS	16.3
BBC 4 × 4 LOS	19.13
BBC 4 × 4 OLOS	30.52
ISM 2 × 2	16.65
ISM 2 × 4	20.1
ISM 3 × 3	23.89
ISM 3 × 4	26.7
ISM 4 × 2	17.92
ISM 4 × 4	31.2
ISM 6 × 8	49.66

[22] The MIMO capacity results were also analyzed to determine the effect of LOS propagation. It was found that in the case of 4 by 4 LOS the capacity was reduced by, as much as 10 b/s/Hz from the average 31.2 b/s/Hz shown in Figure 6a.

4.1.2. Results for Six by Eight Directional Antenna Measurements

[23] The data obtained with the double directional antennas were analyzed for MIMO capacity as displayed in Figure 6d, for correlation at the transmitter and for correlation at the receiver, and for angle of arrival and angle of departure. Correlation analysis showed values between 0.1 and 0.67 at the transmitter with a mean value of $\sim$0.3 and between 0.26 and 0.57 at the receiver with a mean of $\sim$0.42, and mean RMS time delay spread was found to be on the order of 106 ns.

[24] Using the expression for the capacity $C = n \log_2(1 + \frac{\rho}{n}(1 - rc))$ (n is the minimum number of transmit/receive antennas and ρ is the signal-to-noise ratio) given by *Loyka* [2001] for the uniform correlation model $rc = r$, and exponential correlation model $rc = r^2$ and taking the higher mean value of $r = 0.42$ and 30 dB signal-to-noise ratio the corresponding estimated capacities are 39.7 b/s/Hz and 42.7 b/s/Hz, respectively. The model derived by *Loyka* [2001] was based on correlation between antenna elements of linear arrays whereas the arrays used in the present study were directional and mounted on a circle. Therefore, the application of the model to our results is only indicative of the maximum expected capacity. Nevertheless the achieved capacity of 50 b/s/Hz is higher than the maximum capacity of 44.3 b/s/Hz achieved by setting $rc = 0$. This increase can therefore be attributed to the diversity gain of using 8 antennas at the receiver instead of 6 antennas.

[25] Similar to the computations of the RMS delay spread, the RMS angular spread was computed from the angle of departure/angle of arrival and the mean RMS angular spread for 20 dB threshold at both ends of the link was found to be on similar order (68.5° angle of departure) and (69.7° angle of arrival). The correlation coefficient was also computed between the capacity and the RMS angular spread. The results are 0.65 and 0.41 between capacity and angle of departure and capacity and angle of arrival, respectively. Although the mean RMS angular spread is relatively significant the correlation between capacity and RMS angular spread is less obvious with relatively low figures at both ends of the link. Generally for low angular spread it is necessary to increase the separation between the antenna elements. In the simulations conducted by *Shiu et al.* [2000] to study the effect of angular spread and array geometry on capacity, it was concluded that the uniform linear array with broadside angle of arrival gave higher results for capacity than the inline angle of arrival or the hexagonal array. This however, was assuming a single ring model with a high base station and a mobile unit. The high angular spread achieved in the current measurements compensates for the closeness of the antenna elements, which gives a high capacity.

4.2. Results for BBC TV Studios

[26] For the BBC measurements, the data were classified as line of sight versus obstructed line of sight and the results for the 2.25 GHz frequency band are shown in Figure 7. In contrast to the ISM band results the mean RMS time delay spread was 13 ns for the LOS and 26 ns for the OLOS.

[27] The median measured capacity for the different antenna combinations are compared in Table 1 which show a decrease in the capacity for the LOS case, in comparison to the OLOS. The OLOS capacity is close to the IID capacity of 17.97 b/s/Hz and 31.9 bits/s/Hz for 30 dB SNR and for the 2 by 2 and 4 by 4 antenna configurations, respectively. Although the presence of a LOS component enhances the SNR which increases the capacity of a SISO/SIMO channel, the presence of a dominant LOS component results in a relatively small RMS time delay spread which in turn gives lower MIMO channel capacity.

[28] Since the data were collected systematically along a grid, the capacity estimates could be studied for spatial variations. Figure 8 shows the capacity estimates for locations separated by 2 m on an 8 by 8 m grid for both 2 by 2 and 4 by 4 antenna arrays, where spatial variations on the order of 2 to 5 b/s/Hz can be observed. These can result from the presence of obstructions such as furniture or equipment.

4.3. Frequency Selectivity of MIMO Channels

[29] MIMO configurations are currently being deployed for WiMAX systems which employ orthogonal frequency division multiplexing (OFDM) in a bandwidth which varies from 1.25 MHz to 20 MHz in a number of frequency bands in the 2–6 GHz range. For such systems the effect of frequency selectivity has been shown to increase the bit error rate, BER [*Salous et al.*, 2008; *Khokhar and Salous*, 2008]. Two parameters, which can indicate the effect of frequency selectivity on the BER were introduced and these were the level crossing and the average bandwidth of frequency selectivity. The data in the present study were also analyzed to estimate these parameters for the different antenna configurations. Figure 9 displays the number of crossings per MHz and the normalized average bandwidth for which the data fell below a certain level in dB for both the BBC data and for the ISM data. Generally it can be seen that for the BBC studio data more level crossings per MHz were detected than in the ISM data. This is associated with a lower percentage of the bandwidth falling below the same threshold. For multicarrier sys-

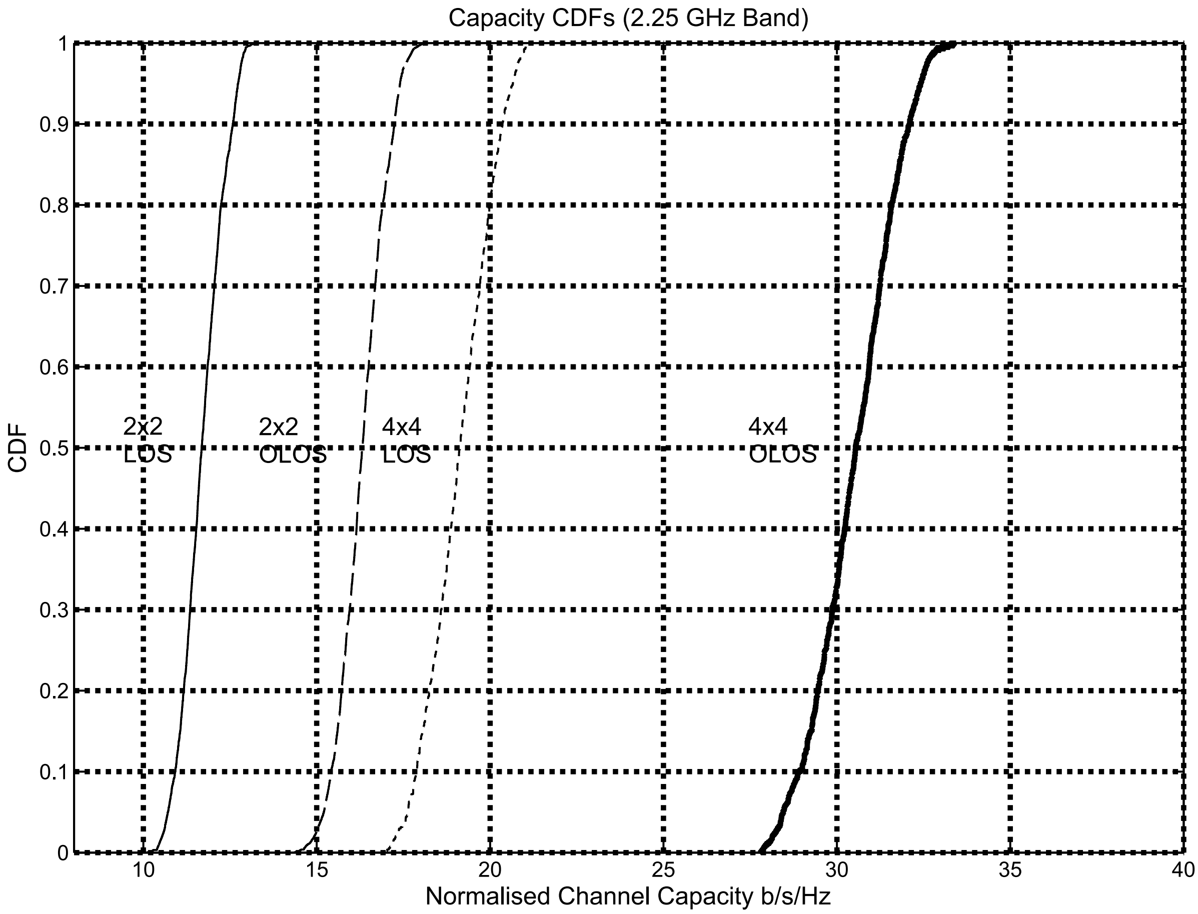

Figure 7. CDF for capacity in the TV studios at 2.25 GHz.

tems, the overall percentage of the bandwidth that falls below a certain level results in a higher BER as more carriers suffer from a low signal level. For the ISM band, around 27% of the bandwidth fell below the 6 dB level in contrast to 21% of the bandwidth for the BBC data.

5. Conclusions

[30] Wideband MIMO measurements in two different environments were performed using a chirp channel sounder with switching at the transmitter and parallel receiver channels. The data were collected with either 96 MHz bandwidth or 240 MHz bandwidth with 4 by 4 uniform linear array or uniform circular array with discone antennas and with 6 by 8 directional antennas. The data were classified in a number of ways, which included LOS versus OLOS, stationary versus moving, and on a spatial grid. The results indicate that the indoor radio channel provides spatial multiplexing capacity close to the ideal except for line of sight situations where a significant drop on the order of 11 bits/s/Hz can result. The high-capacity results were related to the low correlation coefficients on the order of 0.3–0.42 at both ends of the radio link. Angular spread on the order of 68–69° was also estimated from the 6 by 8 data, which showed significant capacity due to both the increase in number of antennas and the diversity gain. The correlation between angular spread and capacity was higher for the angle of departure than the angle of arrival with 0.65 in comparison to 0.42.

[31] The median capacity obtained in the ISM band inside the School of Engineering building at Durham University gave comparable results to the OLOS situation in the TV studios for the same number of antennas. These were 16.32 and 30.54 bits/s/Hz for the TV studio and 16.5 and 31.2 bits/s/Hz for the School of Engineering for the 2 by 2 and 4 by 4 antenna array configurations. The spatial capacity on a 2 by 2 m grid can be significantly varied while the movement of one end of the link results in a higher capacity. Finally the data were analyzed to estimate the frequency selectivity properties,

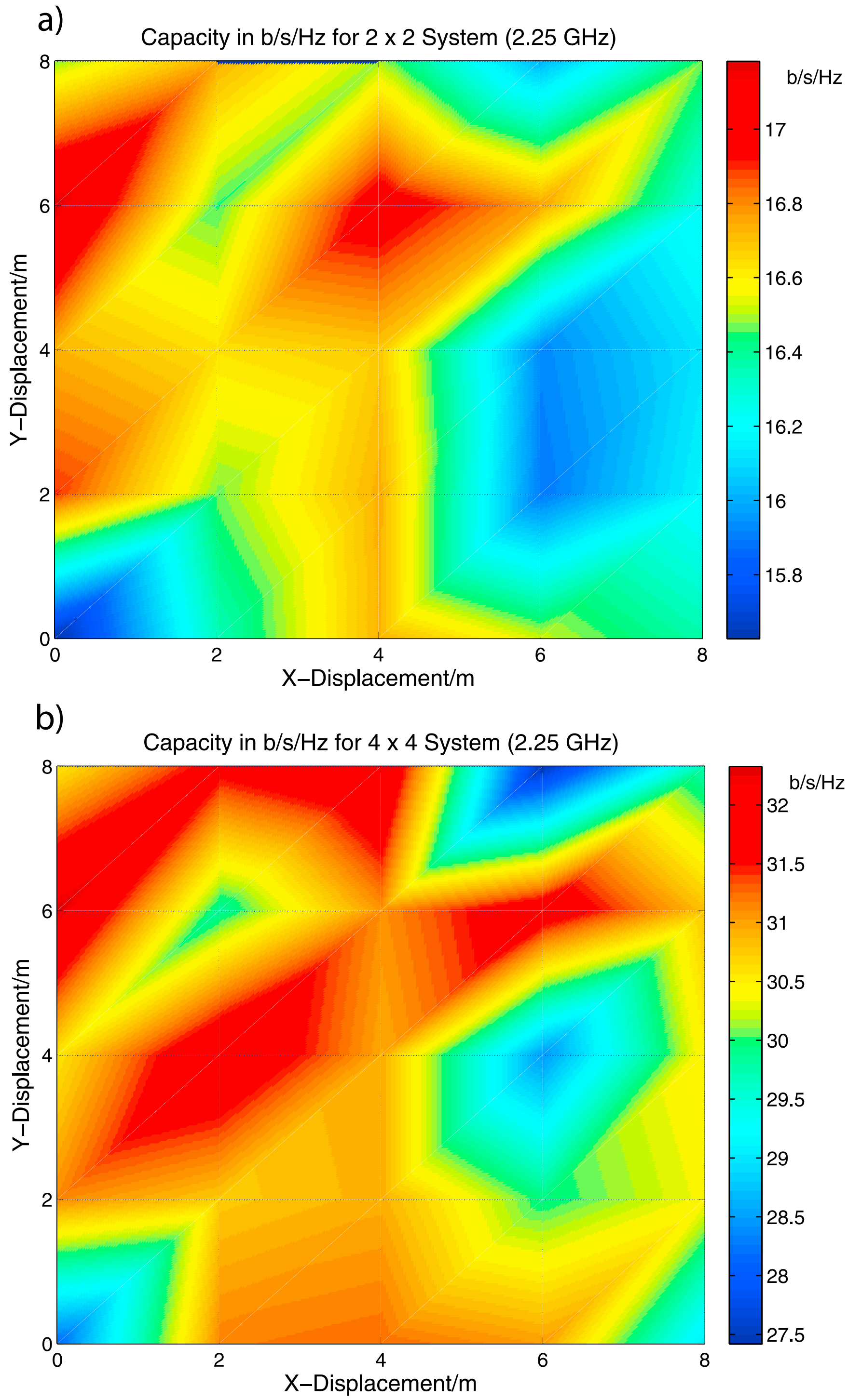

Figure 8. Capacity estimates on 8 m by 8 m grid at 2.25 GHz for (a) 2 by 2 antenna array and for (b) 4 by 4 antenna array.

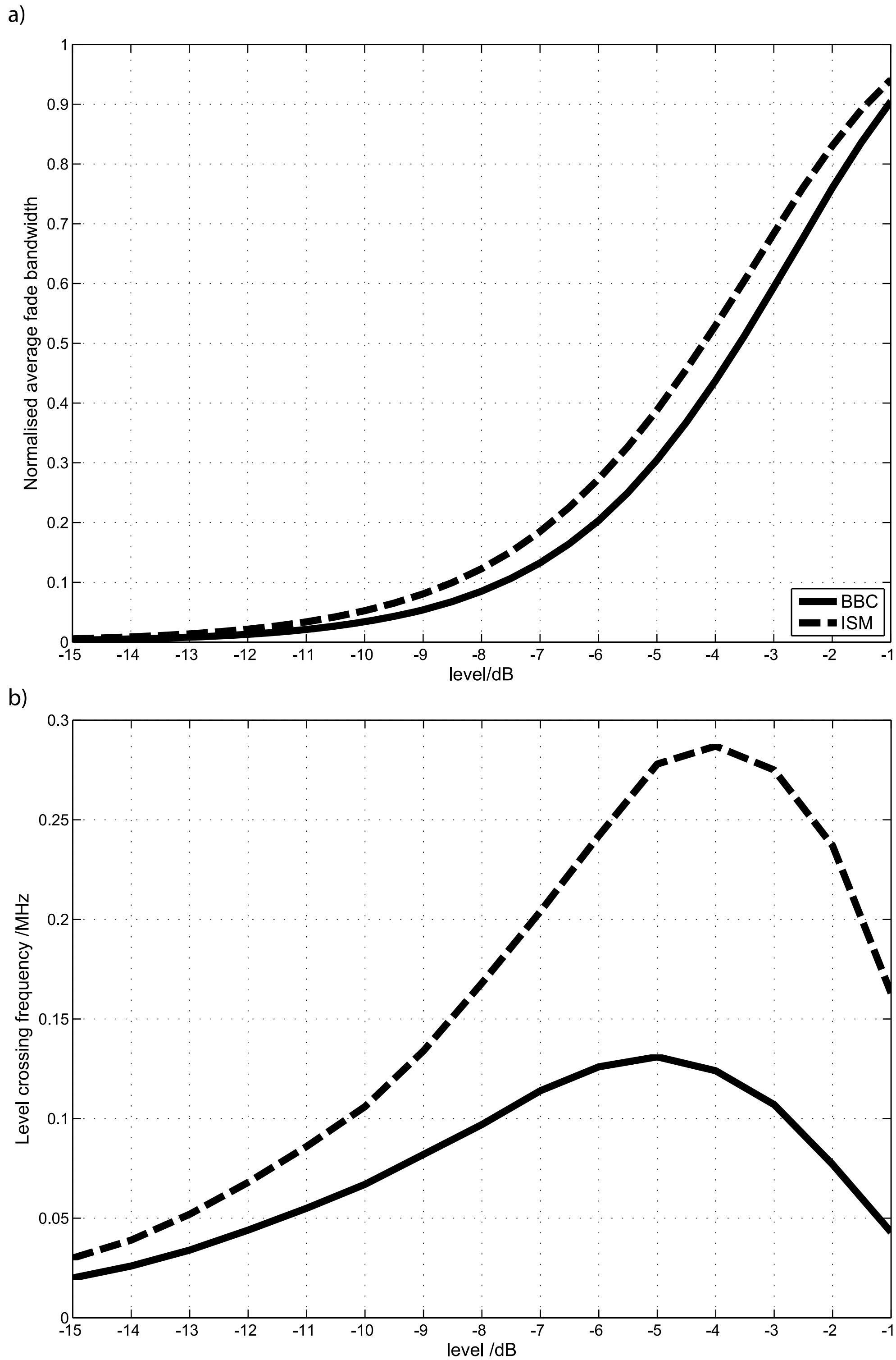

Figure 9. (a) Normalized average bandwidth below a certain level and (b) the corresponding level crossing per MHz for both the ISM band and for the BBC studio environment in the 2.25-GHz band.

which can be used in the design and assessment of OFDM systems.

[32] **Acknowledgments.** The authors would like to thank M. Abdallah, S. M. Feeney, and R. Lewenz for the design of the antenna arrays and their calibration units and the BBC for access to their studios. The sponsorship of N. Razavi-Ghods by EPSRC and the Radiocommunications Agency (now Ofcom) is gratefully acknowledged.

References

Eugene, C. H. Y., K. Sakaguchi, and K. Araki (2004), Experimental and analytical investigation of MIMO channel capacity in an indoor line-of-sight (LOS) environment, in *Proceedings of 15th International Symposium on Personal, Indoor, and Mobile Radio Communications (PIMRC 2004), Barcelona, Spain*, IEEE Press, Piscataway, N. J.

Feeney, S. (2007), *Wideband channel sounding in the bands above 2 GHz*, Ph.D. thesis, Durham Univ., Durham, U. K.

Fleury, B. H., M. Tschudin, R. Heddergott, D. Dahlhaus, and K. I. Pederson (1999), Channel parameter estimation in mobile radio environments using the Sage algorithm, *IEEE J. Sel. Areas Comm.*, *17*, 434–450, doi:10.1109/49.753729.

Foschini, G. F., Jr. (1996), Layered space-time architecture for wireless communication in a fading environment when using multi-element antennas, *Bell Lab. Tech. J.*, 41–59.

Foschini, G. J., and M. J. Gans (1998), On limits of wireless communication in a fading environment when using multiple antennas, *Wirel. Personal Commun.*, *6*, 311, doi:10.1023/A:1008889222784.

Hassibi, B, and B. M. Hochwald (2003), How much training is needed in multiple-antenna wireless links?, *IEEE Trans. Inf. Theory*, *49*, 951–964, doi:10.1109/TIT.2003.809594.

Jenson, M. A., and J. W. Wallace (2004), A review of antennas and propagation for MIMO wireless communications, *IEEE Trans. Antennas Propag.*, *52*(11), 2810–2824, doi:10.1109/TAP.2004.835272.

Khokhar, K., and S. Salous (2008), Frequency domain simulator for mobile radio channels and for IEEE 802.16 standard using measured channels, *IET Commun.*, *2*(7), 869–877.

Loyka, S. (2001), Channel capacity of MIMO architecture using the exponential correlation matrix, *IEEE Commun. Lett.*, *5*(9), 369–371, doi:10.1109/4234.951380.

Loyka, S., and A. Kouki (2001), The impact of correlation on multi-antenna systems performance: Correlation matrix approach, in *Proceedings of 54th VTC Conference*, pp 533–537, IEEE Press, Piscataway, N. J.

Maharaj, B. T., W. Wallace, L. P. Linde, and M. A. Jensen (2005), Frequency scaling of spatial correlation from co-located 2.4 and 5.2 GHz wideband indoor MIMO channel measurements, *IEE Electron. Lett.*, *41*, 336–337, doi:10.1049/el:20057690.

Paulraj, A., R. Nabar, and D. Gore (2003), *Introduction to Space-Time Wireless Communications*, Cambridge Univ. Press, New York.

Salous, S. (1986), An FMCW channel sounder with digital processing for measuring the coherence of wideband HF radio links, *IEE Proc. F.*, *133*(5), 456–462.

Salous, S., and V. Hinostroza (2005), Wideband indoor frequency agile channel sounder and measurements, *IEE Proc. Antennas Propag.*, 573–580, doi:10.1049/ip-map:20041203.

Salous, S., N. Nikandrou, and N. Bajj (1998), Digital techniques for mobile radio chirp sounders, *IEE Proc. Commun.*, *145*, 191–196, doi:10.1049/ip-com:19982078.

Salous, S., P. Filippidis, R. Lewenz, I. Hawking, N. Razavi-Ghods, and M. Abdallah (2005a), Parallel receiver channel sounder for spatial and MIMO characterisation of the mobile radio channel, *IEE Proc. Commun.*, *152*(6), 912–918, doi:10.1049/ip-com:20045346.

Salous, S., S. Feeney, N. Razavi-Ghods, and R. Lewenz (2005b), Measurements in the 2–6 GHz band, paper presented at XXVIIIth General Assembly, Int. Union of Radio Sci., New Delhi, India.

Salous, S., S. M. Feeney, K. Khokhar, and R. Lewenz (2008), Measurements of radio channels and BER estimation of IEEE802.16 standard in semi-rural environment at three frequencies in the 2–6 GHz frequency band, *IET Commun.*

Schwarz, K., U. Martin, and H. W. Schüßler (1993), Devices for propagation measurement in mobile radio channels, in *Proceedings of 4th International Personal, Indoor and Mobile Radio Communications (PIMRC 1993), Yokohama, Japan*, IEEE Press, Piscataway, N. J.

Shiu, D.-S., G. J. Foschini, M. J. Gans, and J. M. Kahn (2000), Fading correlation and its effect on the capacity of multi-element antenna systems, *IEEE Trans. Commun.*, *48*(3), 502–513.

Wallace, J. W., M. A. Jensen, A. L. Swindlehurst, and B. D. Jeffs (2003), Experimental characterization of the MIMO wireless channel: Data acquisition and analysis, *IEEE Trans. Wirel. Comm.*, *2*, 335–343, doi:10.1109/TWC.2003.808975.

Winters, J. H. (1987), On the capacity of radio communication systems with diversity in a Rayleigh fading environment, *IEEE J. Sel. Areas Comm.*, *5*, 871–878, doi:10.1109/JSAC.1987.1146600.

N. Razavi-Ghods, Cavendish Laboratory, University of Cambridge, J. J. Thomson Avenue, Cambridge CB3 0HE, UK.

S. Salous, School of Engineering, Durham University, South Road, Durham DH1 3LE, UK. (sana.salous@durham.ac.uk)